IJST EXPLORE International Journal of Science and Technology
CENTRE OF PROFESSIONAL RESEARCH PUBLICATIONS
ISSN 2049-7318

International Journal of Science and Technology Volume 2 No. 2, February, 2013

Study on Microstructure, Tensile Test and Hardness 304 Stainless Steel Jointed by TIG Welding

Halil İbrahim Kurt[1], Ramazan Samur[2]
[1]Gaziantep Vocational High School, Gaziantep University, Gaziantep-Turkey
[2]Technical Education Faculty, Marmara University, Göztepe-İstanbul-Turkey

ABSTRACT

In this study, microstructure evaluation and mechanical properties of 304 austenitic stainless steels (SS) jointed by tungsten inert gas (TIG) welding by using 308 stainless steel filler wire were examined. Microstructure and mechanical properties (tensile testing and hardness measurement) of the jointed material were investigated. It was observed from the tensile test result that the ultimate tensile strength is 1800 Mpa, yield strength is 75 Mpa, the breaking strength is 1520 Mpa, percent elongation and reduction area are 25%. The hardness values of welding metal (WM), base metal (BM) and HAZ are 233, 321 and 201 HV, respectively. Microstructures of BM, HAZ and WM were studied with scanning electronic microscopy (SEM) and electron dispersive spectrum (EDS) analysis, optical microscopy (OM) and stereo microscopy (SM). In weld metal chromium carbide precipitation was observed. The welding metal contains a dendrite structure (skeletal and lathy ferrite).

Keywords: *TIG Welding, Austenitic Stainless Steel, Tensile Test*

1. INTRODUCTION

TIG welding which uses a non-consumable tungsten electrode and an inert gas for arc shielding is an extremely important arc welding process [1]. In this process, an electric arc is formed between a tungsten electrode and the base metal. The arc region is protected by an inert gas or mixture of gases [2]. Although this type of welding is usually done with a single electrode, it may be sometimes done with several electrodes [3]. In TIG welding, shielding gas plays an important role. Composition of a shielding mixture in arc welding depends mostly on the kind of material to be welded. The selection of the shielding gas should, by all means, take into account chemical–metallurgical processes between the gases and the molten pool that occur during welding [4]. TIG welding quality is strongly characterized by the welding pool geometry. This is because the welding pool geometry plays an important role in determining the mechanical properties of the welding. Therefore, it is very important to select the welding process parameters for obtaining optimal welding pool geometry [5, 6]. Stainless steels were considered to have, in the annealed condition, very good resistance to general and localized corrosion due to their chromium content, which is higher or equal to a critical value around atomic 13 % [7]. Welding together two different parts leads to the selection of materials more adequate to the function of the said part. Nevertheless, welding is recognized as zones which are particularly sensitive to corrosion [8]. Basically, stainless steels may be welded in different ways; of course, it is important to choose the most adequate method to obtain joints of good characteristics.

The main aim of this study is to determine microstructure and mechanical properties of 304 SS material jointed by TIG welding. For this, hardness measurement, microstructures of BM, HAZ and WM and tensile test of 304 SS material jointed by TIG welding were carried out.

2. EXPERIMENTAL MATERIALS AND PROCEDURE

In this study, the 2 mm thick 304 stainless steel plates (100X100X2) and the 2,4 mm thick 308 stainless steel filler wires were used as the welding materials. The compositions of stainless steels were shown in Table 1. In the experiments, Franius Magic Wave 3000 type welding machine was used. The heat generated by the electric arc was used to melt and joint the base metal. Gas shielding for welding was kept in the flowing rate of 17 lit/min. Current intensity and welding speed were chosen as 80 A and 3.5 mm/sec., respectively. During the welding, welding gun was controlled manually and the welding wire was fed manually into the welding area. After welding, specimens were cooled in the air.

Table 1. Chemical compositions of 304 and 308 stainless steels (%) [9]

Materials	C	Mn	Si	Cr	Ni	P	S	Fe
304	0.08	2	1	18-20	8-10.5	0.0045	0.03	Balance
308	0.08	2	1	19-21	10-12	0.0045	0.03	Balance

To observe microstructures, from the specimens were vertically taken cross-sections and after the taken cross-sections were covered by bakelite. After covering, the specimens were sanded with 80-150-400-600- 800-1200 number emery. Standard polishing procedure was used for general microstructural observations [10]. After, polishing was done with broadcloth in alumina solution. The specimens were cauterized as electrolytic. After, microstructures of BM, HAZ, WM and EDS were analyzed. For grain, grain boundary and microstructure analysis of BM, HAZ and WM were used ZEISS 477901-9901 optical microscopy, OLMPUS SZ-PT stereo microscopy and JEOL JSM 5910 LV scanning electron microscopy. To determine the mechanical properties of 304 SS material were done tensile test and hardness measurement. The tensile tests were carried out at room temperature, specifically, the methods of determination of yield strength, tensile strength, elongation, and reduction of area. The tests were carried out x- direction and with INSTRON 1195 tensile testing machine. Load was applied at the rate of 0.5 mm/min. The specimens were prepared according to ASTM E8-04, as shown in Fig. 1 [11]. Vickers hardness measurement was carried out with a DUKON TESTER WILSON device and by applying 200-g load and the specimens were prepared according to ASTM E92-82 [12].

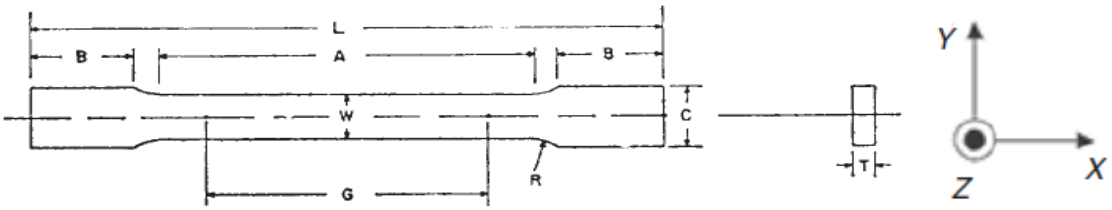

Fig.1. Test Specimen for the Tensile Test

Table 2. Symbols and Dimensions for the Tensile Test

Symbol	Dimension (mm)
T	2
C	10
W	8
G	30
A	48
L	100
R	2
B	25

3. RESULTS AND DISCUSSION

3.1 Tensile and Hardness Properties

The tensile strengths of all joints were evaluated. Three specimens were tested and from this three results were obtained the average tensile strength. The tensile test results of the 304 SS material jointed by TIG welding were given in Table 3.The stress- elongation curve was shown in Fig. 2, and it was plotted from measured load vs. extension values for jointed 304 SS material.

Table 3. Tensile Test Results of 304 SS Jointed by TIG Welding

Ultimate Tensile Strength (Mpa)	Breaking Strength (Mpa)	Elongation (%)	Reduction Area (%)	Yield Strength (Mpa)
1800	1520	25	25	75

Tensile tests provide information on the strength and ductility of materials under uniaxial tensile stresses. This information may be useful in comparisons of materials; alloy development, quality control, and design under certain circumstances. According to Lippold and Kotecki (2005), ultimate tensile strength of 304 SS is 515 Mpa, yield strength is 205 MPa, elongation is percent 40 and reduction area is 50% [13]. Ultimate tensile strength of 304 SS welded with TIG welding method is 1500 Mpa [14]. Kumar and Shahi (2011), found the ultimate tensile strength and percent elongation of 304 SS welded by TIG method at low temperature are 657.32 Mpa and 24.28 %, respectively [15]. The comparison of UTS and elongation values revealed that ultimate tensile strength, percent elongation and breaking strength increased and yield strength and reduction area decreased. The fracture of jointed 304 SS material occurred in HAZ. Like in Fig. 2 shown, fracture which carried out 304 SS material jointed TIG welding is ductile.

The hardness measurements were performed to determine the strength. The hardness profile was carried out as shown in Fig. 3a, where the different main areas of interest were identified, such as the fusion zone (FZ), HAZ and the BM [16]. Fig. 3b shows the trend of the

hardness measurements obtained. Additionally, the values of the hardness were presented at Table 4.

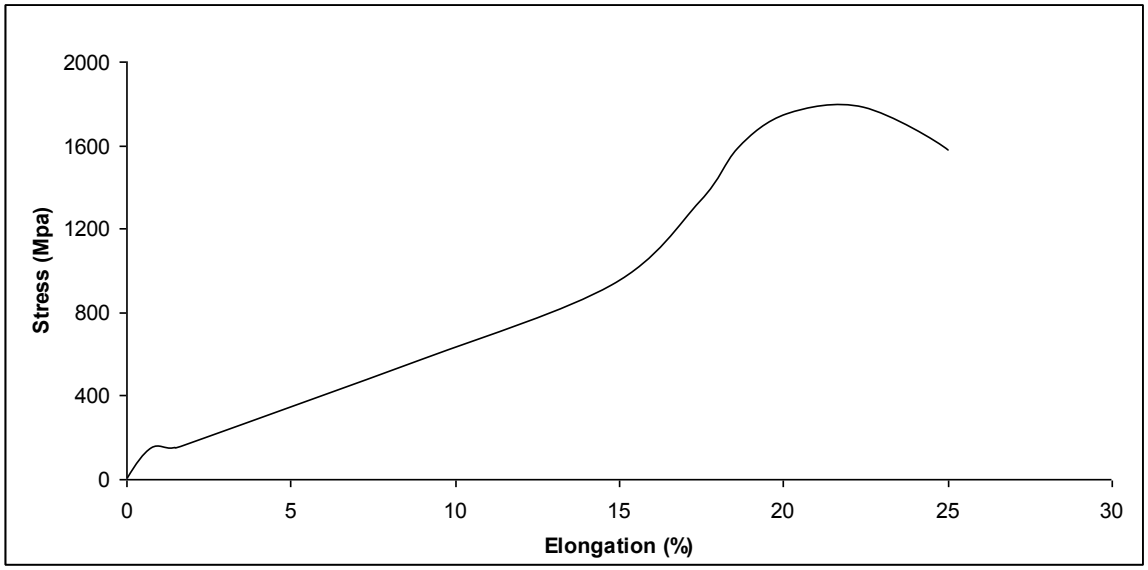

Fig. 2. Tensile Test Graphic of 304 SS Jointed by TIG Welding

Fig. 3b shows a diminution of the hardness from the BM to the FZ which is produced as a consequence of a microstructural change. Moreover, that was observed the decrease in hardness of HAZ, which can be attributing to an increase of the mean grain size after the welding process. It was observed that from BM to the center of the HAZ towards hardness decreased from 321 to 201 HV, from HAZ to the center of the WM towards hardness increased from 201 to 233 HV. Kumar and Shahi (2011), found the hardness of WM 205 HV, respectively [15]. Coarse grained structure in HAZ occurred, the hardness of HAZ affected negatively. Therefore, micro-hardness of HAZ decreased as to BM and WM. As shown in Fig. 5, the hardness of WM is higher than HAZ and lower than BM.

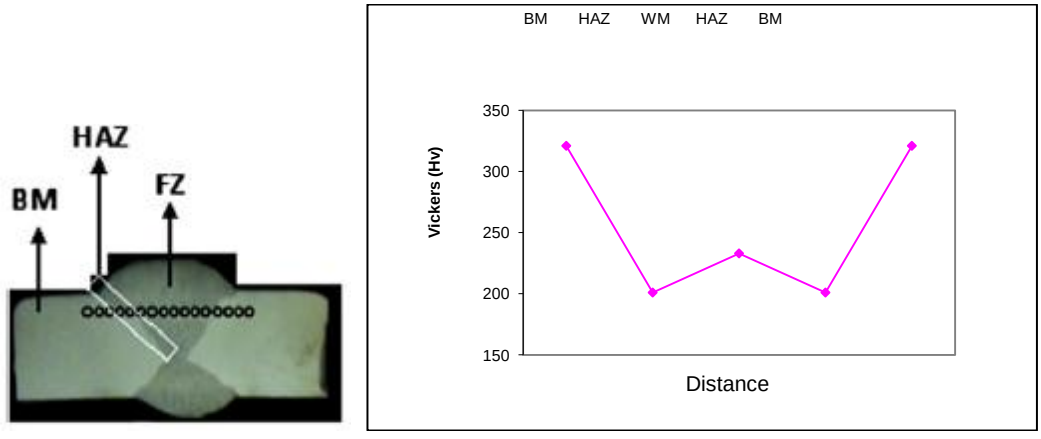

(a) (b)

Fig. 3. Vickers Hardness, (a) Profile Scheme of the Hardness (b) Graphic of the Hardness Measured

Table 4. Micro-hardness Values of Welded Stainless Steel

BM	HAZ	WM
321	201	233

3.2 Microstructure Properties

Full penetration joints were produced with TIG welding. Fig. 4a shows the morphology of the base material, which evidence the austenitic-grain microstructure of an AISI/SAE 304 stainless steel. Additionally, for the TIG welding processes, the microstructural analysis was carried out at the fusion zone (FZ), or the center of the welding. Fig. 4b presented an austenitic, Lathy and skeletal (vermicular) ferrite microstructure for the TIG process. The lathy-ferrite microstructure can emerge due to greater ferrite contents and/or a characteristic cooling time after the welding procedure steel [17-19].

The metallographic analyses of the welding processes were performed at the cross-section area of the welding specimens. The weld heat input conditions in this study were lower than other studies because of the weld cracking susceptibility of type 304 SS becoming sensitive. The cracking susceptibility was mitigated by the weld heat input reduction [20].

Fig. 5a shows the optic micrograph of HAZ and WM. Dendrites can be observed extending from the fusion boundary to the weld centerline. The cooling rate at the edges is higher than in the middle of the welding and, therefore, the rate of edge scale formation is slower than in the middle of the welding. The change in scale morphology can be ascribed to an edge effect phenomenon occurring during the cooling of the material. Fig. 5b shows the stereo micrograph of WM, HAZ and BM. The parent material, HAZ and FZ could be discriminated easily. In welding zone, a small amount chromium carbide precipitation is to be formed. According to welding metal external surface, center of welding metal were exposed to more heat. Fig. 5c shows scanning electron microscopy micrographs of HAZ and BM. Fig. 6a shows electron dispersive spectrum (EDS) analysis and Fig. 6b shows scanning electron microscopy micrograph of WM. Dendrite cells could be discriminated easily.

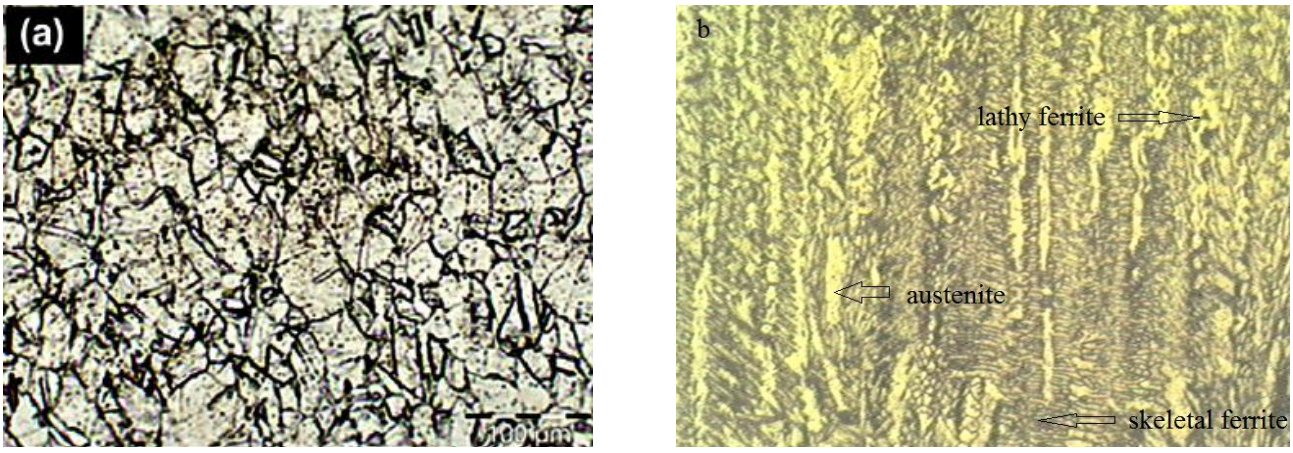

Fig. 4. Micrographs of the Microstructures, (a) BM (b) TIG Welding at the Fusion zone (X200)

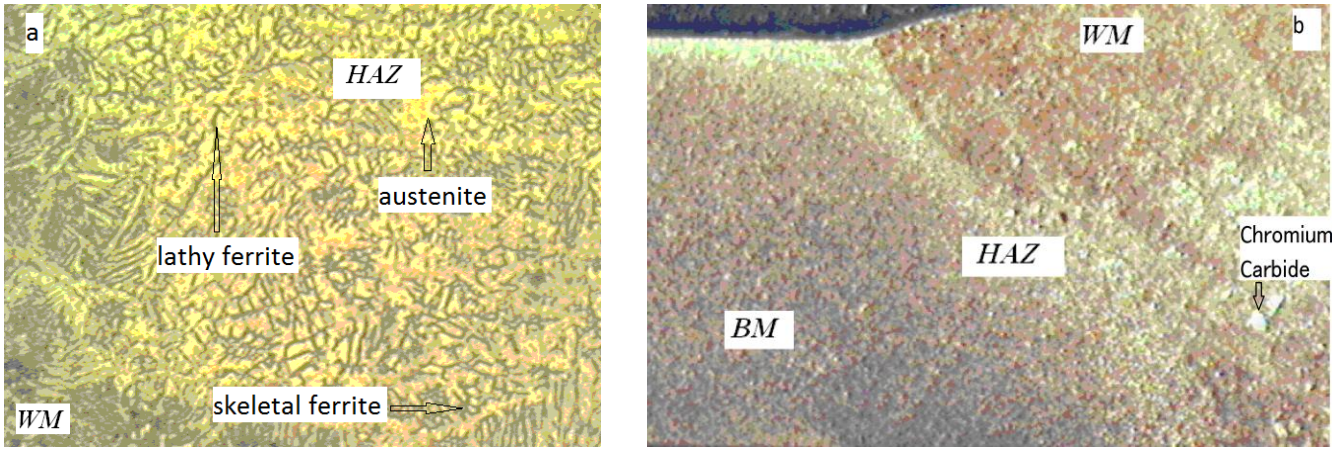

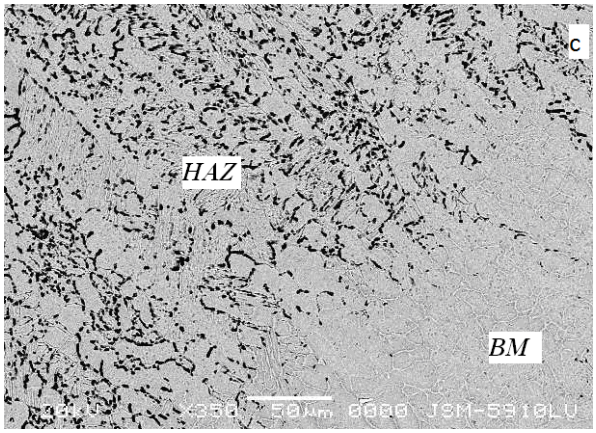

Fig. 5(a) Optical Micrographs of HAZ and WM (X200), (b) Stereo Micrographs of HAZ, WM and BM (X200), (c) SEM Micrographs of HAZ and BM (X350)

Results of EDS analysis were shown in Table 5. In Fig. 5c, the BM and HAZ can be observed obviously. There is a dendrite structure in Fig. 5c. The dendrite structure is going to welding metal and this at the same time was shown in Fig. 5a. HAZ is composed of dark dendrite structure in austenite matrix in Fig. 5c and this at the same time was shown in Fig. 6. In Figure 5c and Fig 6a, white zone is austenite and dark zone is ferrite. Fig. 5(c) shows that dendrites can be observed extending from the fusion boundary to the weld centerline.

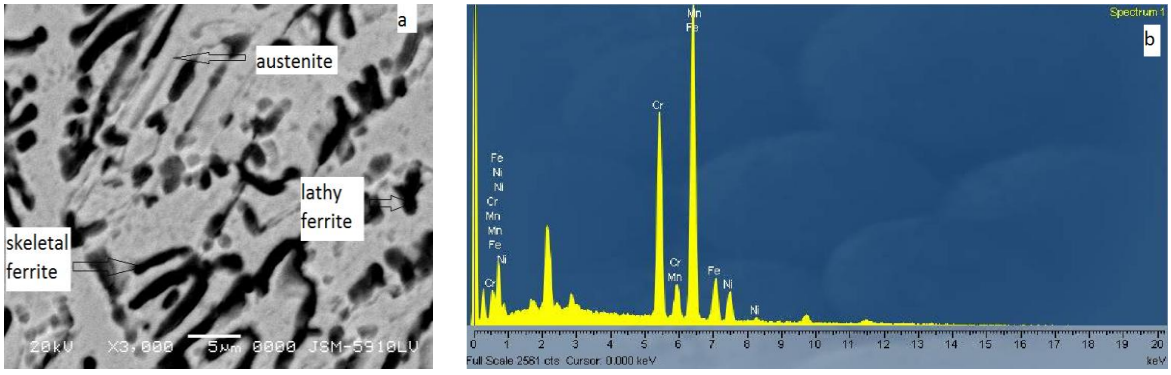

Fig. 6 SEM Micrographs and EDS Analysis of WM (X3000)

Table 5. EDS Analysis of WZ

Spectrum	Cr	Mn	Fe	Ni	Si	P	S	C	Total
Spectrum 1	18,74	1,43	68,479	10,28	0,93	0,039	0,029	0,073	100.00
Max.	18,74	1,43	68,479	10,28	0,93	0,039	0,029	0,073	100,00
Min.	18,74	1,43	68,479	10,28	0,93	0,039	0,029	0,073	100,00

4. CONCLUSION

The tensile test, microstructure and hardness measurement were studied over 304 stainless steel materials jointed by TIG welding. According to base metal, hardness value of welding zone decreased and the value of welding zone is higher heat affected zone. Coarse grained structure in HAZ occurred, the hardness of HAZ affected, negatively. The tensile strength, yield strength and elongation are 1800, 75 Mpa and 25%, respectively. The failure started via crack in heat affected zone and fracture carried out in heat affected zone. Fracture which carried out 304 SS material jointed TIG welding is ductile. Fracture of the specimens showed an intergranular fracture. Microstructure analyses reveal austenite, lathy ferrite and skeletal ferrite. Transition zone or HAZ demonstrates obviously a dendrite structure.

REFERENCES

[1] Juang S.C., Tarng Y.S., *Process parameter selection for optimizing the weld pool geometry in the tungsten inert gas welding of stainless steel*, J. Mater Process Tech., 122(1) (2002) 33 – 37.

[2] Cary H.B., 2nd ed. *Modern welding technology*, AWS, (1981) p. 82 –85.

[3] Minnick W.H., *Gas tungsten arc welding handbook*, The Good heart-Willcox Company, Inc.,(1996)

[4] Suban M., Tusek J., *Experimental research of the effect of hydrogen in argon as a shielding gas in arc welding of high alloy stainless steel*, Int. J. Hydrogen Energy, 25(4) (2000) 369 – 376.

[5] Lucas J., Fang M.T.C., Zeng X.M., *Use of neural networks for parameter prediction and quality inspection in tungsten inert gas welding*, Trans. Inst. Measur. Contr., 15 (2) (1993) 87–95.

[6] Tsai H.L., Yeh S.S., Tarng Y.S., *Modeling, optimization and classification of weld quality in TIG welding*, Int. J. Mach. Tools Manuf., 39 (1999) 1427–1438.

[7] Sahlaoui H., Sidhom H., Philibert J., Makhlouf K., *Effect of ageing conditions on the precipitates evolution, chromium depletion and intergranular corrosion susceptibility of AISI 316L*, experimental and modeling results, Materials Science & Engineering, 372 (2004) 98–108.

[8] Meyer J.-M., Reclaru L., Eschler P.Y., Lerf R., *Corrosion behavior of a welded stainless-steel orthopedic implant*, Biomaterials, 22 (2001) 269–279.

[9] Fuller R.W., Ehrgott Jr J.Q.., Heard W.F., Robert S.D., Stinson R.D., Solanki K., Horstemeyer M.F., *Failure analysis of AISI 304 stainless steel shaft*, Engineering Failure Analysis, 15 (2008) 835–846.

[10] ASTM International E407-07, *Standard practices for micro-etching metal and alloys.*

[11] ASTM, E 8 – 04, *Standard Test Methods for Tension Testing of Metallic Materials.*

[12] ASTM, E 92-82, *Standard Test Method for Vickers Hardness of Metallic Materials.*

[13] Lippold JC, Kotecki DJ., Welding *metallurgy and weldability of stainless steels*, New Jersey: Wiley Inter-Science,(2005).

[14] ASM İnternational Metals Handbook *Properties and Selection: Nonferrous Alloys and Special-Purpose Materials*, (1990) volume 2.

[15] Kumar S., Shahi A.S., *Effect of heat input on the microstructure and mechanical properties of gas tungsten arc welded AISI 304 stainless steel joints*, Materials and Design 32 (2011) 3617–3623.

[16] Galvis A. R., Hormaza E, W., *Characterization of failure modes for different welding processes of AISI/SAE 304 stainless steels*, Engineering Failure Analysis 18 (2011) 1791–1799.

[17] Davis JR., *ASM specialty handbook stainless steel*, ASM International, (1994).

[18] Rajasekhar K., *Microstructural evolution during solidification of austenitic stainless steel weld metals: a color metallographic and electron microprobe analysis study*, Mater Charact, 38(2) (1997) 53–65.

[19] Lakshminarayanan AK, Balasubramanian V, Shanmugam K, *Effect of welding processes on tensile, impact, hardness and microstructure of joints madeof AISI 409 FSS base metal and 308L ASS filler metals*, Iron mak steel mak., (2009)75–80.

[20] Morishima Y., Koshiishi M., Kashiwakura K., Hashimoto T., Kawano S., *Re-weldability of neutron irradiated Type 304 and 316L stainless steels*, Journal of Nuclear Materials 329–333 (2004) 663–667.